Quantitative Salivary Gland Scintigraphy

S. Klutmann, K.H. Bohuslavizki, S. Kröger, C. Bleckmann, W. Brenner, J. Mester and M. Clausen

Department of Nuclear Medicine, University Hospital Eppendorf, Hamburg; and Clinic of Nuclear Medicine, Christian-Albrechts-University, Kiel, Germany

Objective: Uptake of ^{99m}Tc-pertechnetate in salivary glands reflects intact salivary gland parenchyma. However, no standardized protocol for an accurate quantification of parenchymal function has been established so far.
Methods: In this paper we report on a validated acquisition protocol supplying a normal database for standardized quantitative salivary gland scintigraphy.
Results: The major advantage of salivary gland scintigraphy, as compared to other imaging modalities, is that both parenchymal function and excretion fraction of all four major salivary glands (i.e., parotid and submandibular glands) can be simultaneously quantified with a single intravenous injection.
Conclusion: Quantitative salivary gland scintigraphy is demonstrated to be a suitable imaging modality for research applications in evaluating the effects of radioprotective drugs on salivary glands. Salivary gland scintigraphy is easy to perform, reproducible and well-tolerated by the patient.
Key Words: salivary gland scintigraphy; Sjögren's syndrome; sialolithiasis; xerostomia; normal database; research of radioprotection; amifostine

J Nucl Med Technol 1999; 27:20–26

Several modalities are known for salivary gland imaging, such as sonography, sialography, scintigraphy, CT and MRI. The advantages and disadvantages of these different imaging modalities are listed in detail in Table 1. CT and MRI are well-established in oncological settings because of their high geometric resolution and their well-known differentiation of soft tissue from osseous structures. Sonography allows a noninvasive, reproducible evaluation of the salivary gland's morphology with high-detail resolution and easy detection of sialolithiasis. Sialography is well-established in the diagnosis of functional obstruction, but cannulization of all four salivary gland ducts is difficult to perform and often painful for the patients. Neither sonography nor sialography allow quantification of the salivary gland's function and obstruction. This quantification is in principle feasible by measuring the saliva drainage, the so-called sialometry. However, the cannulization of all salivary gland ducts is mandatory as well and, therefore, sialometry has not become a widespread clinical routine.

Salivary gland scintigraphy using ^{99m}Tc-pertechnetate is based both on its 1-fold negative charge and its similar diameter to chloride yielding corresponding physico-chemical characteristics. Uptake of ^{99m}Tc-pertechnetate in salivary glands reflects intact salivary gland parenchyma. The major advantage of salivary gland scintigraphy, as compared to other imaging modalities, is that both parenchymal function and excretion function of all salivary glands can be quantified simultaneously with a single intravenous injection. Moreover, salivary gland scintigraphy is easy to perform, reproducible and well-tolerated by the patient.

The clinical impact of salivary gland scintigraphy has been reported in several clinical settings, such as Sjögren's syndrome (*1–9*), after multiple high-dose radioiodine treatments (*10–12*), after external irradiation (*13*), and assessment of salivary duct obstruction (*14–19*). Since salivary gland scintigraphy, performed in a qualitative manner, does not confirm minor parenchymal damage, several methods of quantifying parenchymal function have been reported (*8,19–29*). However, none of these methods has been established so far. Some authors (*30–31*) have suggested the quantification of ^{99m}Tc-pertechnetate uptake in salivary glands as a parameter for parenchymal function (*11–12,15–16,32–38*). References for the parenchymal function and saliva excretion in healthy individuals ranged up to 300%, which was mainly due to different accumulation times from 3 min up to 1 h postinjection, a small number of patients, as well as a lack of selection criteria for the healthy individuals studied.

Quantitative salivary gland scintigraphy recently has been standardized (*39–43*). In this paper we report both on a validated acquisition protocol and a normal database for standardized quantitative salivary gland scintigraphy. The diagnostic impact of quantitative salivary gland scintigraphy is reviewed in several clinical settings, such as ongoing Sjögren's syndrome, sialolithiasis with or without parenchymal damage, and parenchymal impairment after radioiodine treatment. Moreover, quantitative salivary gland scintigraphy has been demon-

For correspondence or reprints contact: Karl H. Bohuslavizki, MD, Dept. of Nuclear Medicine, University Hospital Eppendorf, Martinistr. 52, D-20246 Hamburg, Germany.

TABLE 1
Advantages and Disadvantages of Salivary Gland Imaging Modalities

Imaging modality	Advantages	Disadvantages
Sonography	Noninvasive Easy detection of sialolithiasis No radiation burden Reproducible High-detail resolution	No quantification of function No quantification of obstruction
Sialography	Easy detection of sialolithiasis	No quantification of function No quantification of obstruction Difficult to perform Often painful Cannulization of all salivary ducts obligatory
Sialoscintigraphy	Quantification of function Quantification of obstruction Reproducible Well-tolerated Easy to perform	No morphological presentation Radiation burden
Computer tomography	Widespread clinical routine High geometric resolution Differentiation of soft tissue versus osseous structures	No quantification of function Radiation burden
Magnetic resonance imaging	High geometric resolution Differentiation of soft tissue versus osseous structures No radiation burden	No widespread clinical routine No quantification of function Expensive

strated to be a suitable imaging modality for research applications in evaluating the effects of radioprotective drugs on salivary glands.

METHOD OF SALIVARY GLAND SCINTIGRAPHY

The patient is positioned supine, as shown in Figure 1. After intravenous injection of 40–150 MBq ^{99m}Tc-pertechnetate, sequential images of 1 min each are acquired up to 25 min on a large field-of-view gamma camera equipped with a low-energy, high-resolution, parallel-hole collimator. Images are stored in a 128 × 128 matrix. Fifteen minutes postinjection 3 mL of lemon juice are administered intraorally as sialogogum. The patient is told to distribute the lemon juice around his mouth and then swallow it to achieve maximum stimulus on salivary gland excretion (*39–40,42–46*). The effective equivalent radiation dose to the patient is between 0.4–1.6 mSv according to ICRP 53 (*47*).

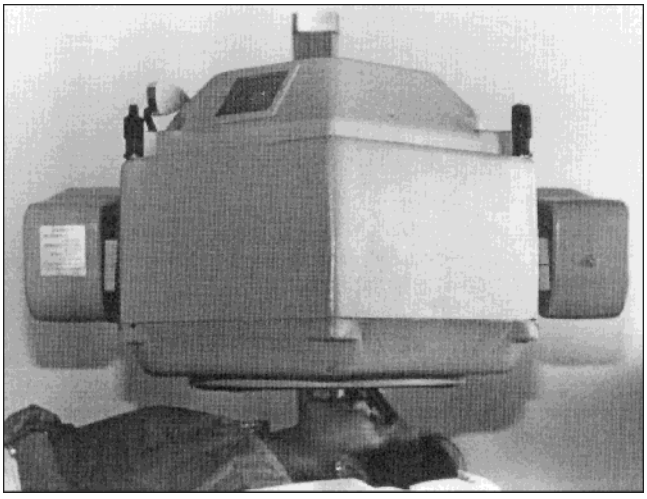

FIGURE 1. Patient's supine position for salivary gland scintigraphy with a slightly reclined head under a large field-of-view gamma camera.

Regions of interest (ROIs) used for quantification include one rectangular background ROI located over the brain and four oval ROIs positioned over both parotid and submandibular glands (*38–40,42–43,48*). ROIs are depicted in Figure 2.

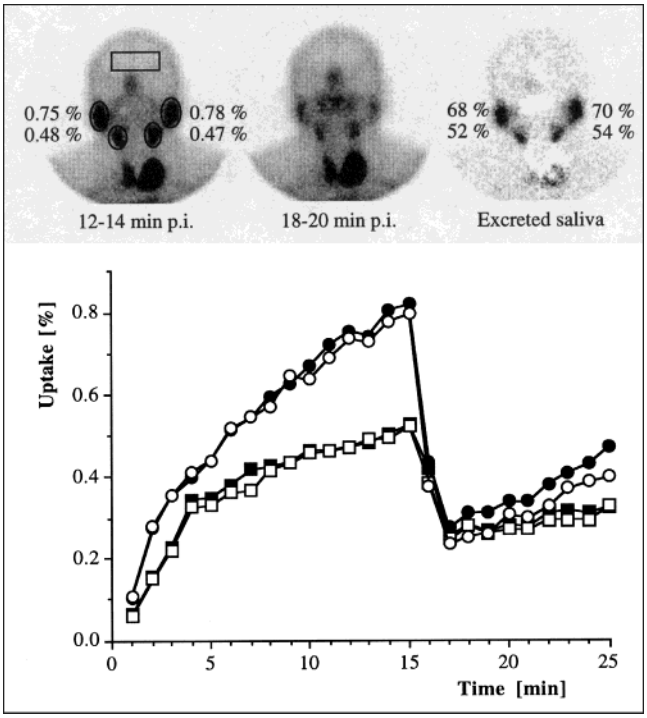

FIGURE 2. Quantitative salivary gland scintigraphy of a healthy individual before applying lemon juice at 12–14 min postinjection, after applying lemon juice at 18–20 min postinjection with a parametric difference image visualizing drained saliva. ROIs used for quantification are depicted on the left scintigram. Numbers on the left image represent uptake of ^{99m}Tc-pertechnetate in percentage of the activity in the submandibular and parotid glands, respectively. Numbers on the right figure represent the excretion fraction of the submandibular and parotid glands, respectively. Time-activity curves of the right (open symbols) and left (filled symbols) parotid gland (circles) and submandibular gland (squares) are demonstrated in the lower row.

Uptake of ^{99m}Tc-pertechnetate was calculated in percentage of the activity injected according to Equation 1:

$$\text{Uptake [\%]} = \frac{\text{count of gland} \cdot \text{calibration factor}}{\text{activity injected}} \cdot 100. \quad \text{Eq. 1}$$

Uptake of ^{99m}Tc-pertechnetate was averaged from 12–14 min postinjection ($U_{12–14}$), and from 18–20 min postinjection ($U_{18–20}$) to reduce noise. Parenchymal function then is reflected by $U_{12–14}$ and excretion fraction was calculated analogous to the ejection fraction of the heart according to Equation 2:

$$\text{EF [\%]} = \frac{U_{12–14} - U_{18–20}}{U_{12–14}} \cdot 100. \quad \text{Eq. 2}$$

NORMAL DATABASE

In this study 723 women and 329 men, aged 18–84 y, had salivary gland scintigraphy before routine thyroid gland scintigraphy. All patients in whom an impairment of salivary gland function was expected were excluded from the study. Impairments included anamnesis of xerostomia, sialolithiasis, external irradiation of the head and neck region, radioiodine treatment, salivary gland tumors, acute or chronic inflammation of the salivary glands, rheumatic disorders, treatment with perchlorate, neuroleptica or antidepressive treatment with anticholinergic side effects, or sonographical or radiological signs of obstruction or parenchymal damage (*39,42–43*).

Finally 312 patients were included in the normal database consisting of 216 women and 96 men with a mean age of 57.4 y and ranging from 18–84 y. The uptake of ^{99m}Tc-pertechnetate was independent of gender and age, and was not side-related. Measurements of left and right salivary glands were summarized. The mean and standard deviation of ^{99m}Tc-pertechnetate uptake and excretion fraction are listed in detail in Table 2. The lower limit of ^{99m}Tc-pertechnetate uptake as a parameter for normal parenchymal function was 0.17% and 0.15% for parotid glands and submandibular glands, respectively. The lower limit of excretion fraction was 28.3% and 20.7% for parotid glands and submandibular glands, respectively (Fig. 2).

TABLE 2
Reference Values for Technetium-99m-Pertechnetate Uptake and Excretion Fraction of Parotid and Submandibular Glands

	Parotid glands	Submandibular glands
Uptake,* x ± s	0.45 ± 0.14	0.39 ± 0.12
Uptake, lower limit	0.17	0.15
Excretion fraction,† x ± s	49.5 ± 10.6	39.1 ± 9.2
Excretion fraction, lower limit	28.3	20.7

*Uptake in percentage of injected activity.

†Excretion fraction in percentage of uptake.

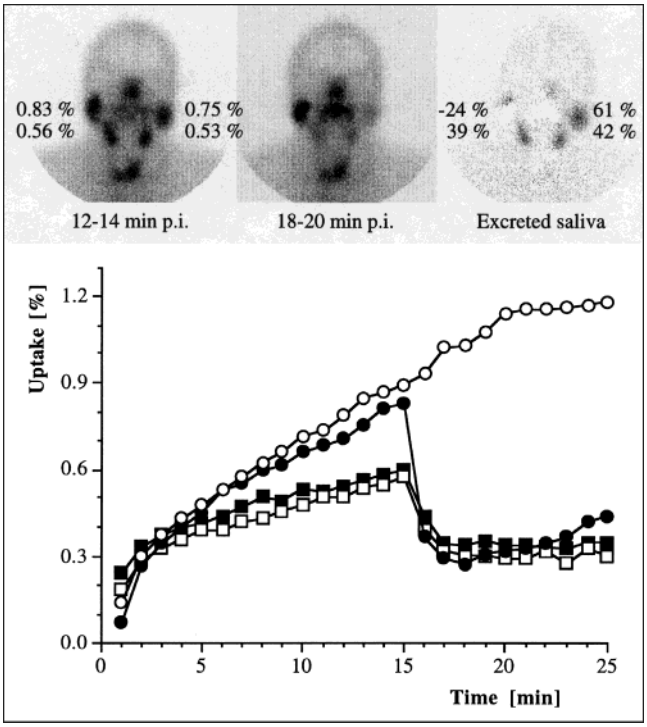

FIGURE 3. Sialolithiasis with functional obstruction of the right parotid gland without any parenchymal impairment. Symbols and numbers are as described in Figure 2. Note the negative number of the excretion fraction of the right parotid gland.

INDICATIONS

Obstruction With or Without Parenchymal Damage

An established indication for salivary gland scintigraphy is for the diagnosis of a functional obstruction in the case of sialolithiasis. (*4,6,14–18,28*). If an additional quantitative measurement is performed, the amount of parenchymal impairment can be evaluated sufficiently. These results may help the clinician make therapeutic decisions for the individual patient:

In case of normal parenchymal function, marsupiliation and removal of the sialolith is performed (Fig. 3).

In case of long-lasting obstruction with subsequent severe parenchymal damage, a resection of the salivary gland is usually preferred (Fig. 4).

Diagnosis of Sjögren's Syndrome

Sjögren's syndrome is a chronic progressive autoimmune disease with lymphocytic infiltration of various exocrine glands. At least two of the following three criteria are required to establish final diagnosis of Sjögren's syndrome: (a) ceratoconjunctivitis sicca; (b) a connective tissue disease; or (c) xerostomia (*6,34*). For the proof of ophthalmic (*9*) and rheumatic (*49–50*) findings, clear criteria have been established whereas quantitative assessment of xerostomia remains difficult.

The additional value of quantitative salivary gland scintigraphy in diagnosing ongoing Sjögren's syndrome was reported recently (*40*). Thirteen patients suspected for Sjögren's syndrome had standardized, quantitative salivary gland scintigra-

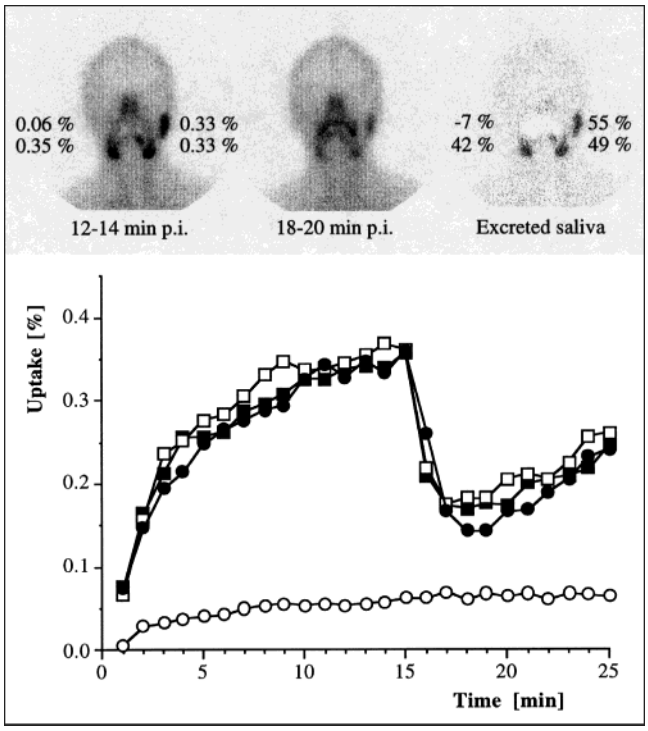

FIGURE 4. Sialolithiasis with functional obstruction of the right parotid gland with subsequent parenchymal destruction. Symbols and numbers are as described in Figure 2. Note missing parenchymal function of the right parotid gland.

phy. Four of the 13 patients showed a slight but statistically significant impairment of parenchymal function. Thus, in these patients quantitative salivary gland scintigraphy led to the finding of one of the criteria, which helped to establish final diagnosis of Sjögren's syndrome in these patients (Fig. 5).

Parenchymal Damage After Radioiodine Treatment

Salivary gland impairment after multiple high-dose radioiodine treatment is a well-known long-term side effect for patients with differentiated thyroid cancer (*10–12*). However, a statistically significant parenchymal impairment was reported after even low-dose radioiodine therapy. The mean reduction of parenchymal function in salivary glands increased from 15% after the administration of as little as 0.4–0.6 GBq ^{131}I through 30% after the application of 1.4–1.5 GBq ^{131}I up to 90% after 24 GBq ^{131}I were administered cumulatively (*43*). Clinical symptoms of xerostomia were recognized at a reduction of parenchymal function of as little as 30% (*42*). Thus, salivary gland scintigraphy allows quantitative evaluation of parenchymal impairment of salivary glands in patients treated with high-dose radioiodine for differentiated thyroid cancer, and these changes are in accordance with clinical symptoms, such as xerostomia as a well-known, long-term side effect.

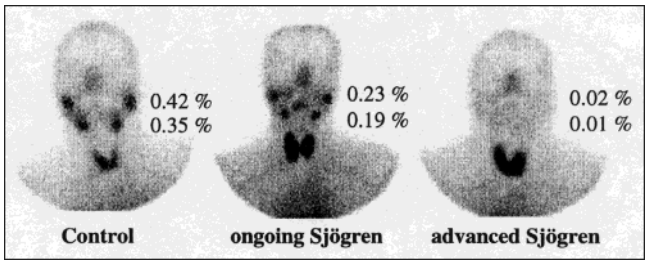

FIGURE 5. Quantitative salivary gland scintigraphy of a healthy control, of patients with beginning and severe Sjögren's syndrome. Numbers on scintigrams represent ^{99m}Tc-pertechnetate uptake in percentage of the activity in submandibular and parotid glands, respectively. Note the parenchymal impairment of all salivary glands in beginning and advanced Sjögren's syndrome.

Research Applications

Protection of salivary gland function has been the focus of ongoing research in patients with head and neck cancer in the last few years. Amifostine, an organic thiophosphate, is the first in about 20 y of a new class of drugs known as cytoprotective agents. Preclinical studies demonstrated both short- and long-term radiation protection by amifostine against radiation-induced damage (*51–58*) since amifostine is markedly accumulated in salivary glands. These promising results were evaluated both in animal experiments and in a prospective patient study.

A total of 15 male New Zealand White rabbits received 2 GBq ^{131}I intravenously to ablate the thyroid and to significantly impair the parenchymal function of the salivary glands. Rabbits were divided into two groups: 10 rabbits received 200 mg/kg amifostine (Ethyol®, Essex, München, Germany) intravenously and 5 rabbits served as controls receiving physiological saline solution before high-dose radioiodine treatment. Salivary gland parenchymal function was quantified using standardized quantitative salivary gland scintigraphy before and at 4-wk intervals up to 24 wk after the application of ^{131}I, as described in detail previously (*42–43,48,59*).

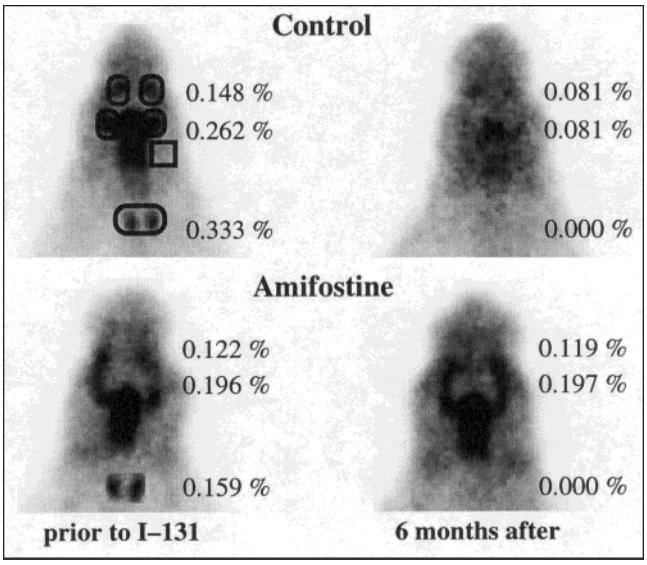

FIGURE 6. Salivary gland scintigraphy of an untreated rabbit (upper row) and of a rabbit treated with 200 mg/kg amifostine (lower row) before and 6 mo after application of 2 GBq ^{131}I. Numbers represent uptake of ^{99m}Tc-pertechnetate in percentage of the activity in the submandibular, parotid and thyroid glands, respectively. Note complete ablation of the thyroid gland in both rabbits while marked parenchymal impairment of submandibular and parotid glands is detected in the untreated rabbit only.

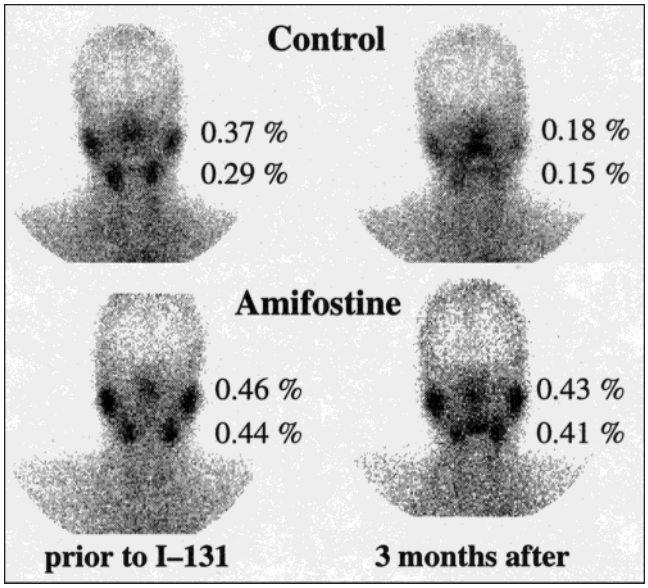

FIGURE 7. Salivary gland scintigraphy of an untreated patient (upper row) and of a patient treated with 500 mg/m^2 amifostine (lower row) before and 3 mo after administration of 6 GBq ^{131}I. Numbers represent uptake of ^{99m}Tc-pertechnetate in percentage of the activity in the submandibular, parotid and thyroid glands, respectively. Note complete ablation of the thyroid gland in both patients while marked parenchymal impairment of submandibular and parotid glands is detected in the control patient only.

Before high-dose radioiodine treatment, thyroid uptake was 0.419 in control and amifostine-treated rabbits. Four weeks after high-dose radioiodine treatment, complete ablation of the thyroid gland was achieved in both groups (Fig. 6). This is an inevitable prerequisite for the application of amifostine in differentiated thyroid cancer since both normal and malignant transformed thyroid tissues must be destroyed sufficiently by radioiodine. Before high-dose radioiodine treatment, uptake of ^{99m}Tc-pertechnetate in 5 control rabbits versus 10 amifostine-treated rabbits was neither significantly different in the parotid glands nor in the submandibular glands. In control rabbits, 12 wk after high-dose radioiodine treatment parenchymal function was reduced significantly ($P < 0.0001$) by 52% and 30%, and 24 wk after high-dose radioiodine treatment by 75% and 54% in the parotid and submandibular glands, respectively (Fig. 6). In contrast, in amifostine-treated rabbits 12 wk after high-dose radioiodine treatment parenchymal function was reduced by 7% and 5% ($P > 0.05$), and 24 wk after high-dose radioiodine treatment by 11% and 7% ($P < 0.01$) in the parotid and submandibular glands, respectively (Fig. 6). Histopathologically, marked lipomatosis was observed in control animals but was negligible in amifostine-treated animals.

Moreover, quantitative salivary gland scintigraphy was performed prospectively in 42 patients with differentiated thyroid cancer before and 3 mo after high-dose radioiodine treatment with 6 GBq ^{131}I in a double-blind, placebo-controlled study. Twenty-two patients were treated with 500 mg/m^2 amifostine intravenously before high-dose radioiodine treatment, and 20 patients served as controls. Parenchymal function was evaluated quantitatively as uptake of ^{99m}Tc-pertechnetate in percent of the activity injected. Xerostomia was graded according to WHO criteria. In 20 control patients high-dose radioiodine treatment significantly impaired ($P < 0.001$) parenchymal function by 35% and 38% in parotid and submandibular glands, respectively (Fig. 7). Eight of the 20 patients developed Grade I (WHO) xerostomia. In contrast, there was no significant decrease ($P = 0.981$) in parenchymal function in amifostine-protected patients (Fig. 7), and xerostomia did not occur in any of them.

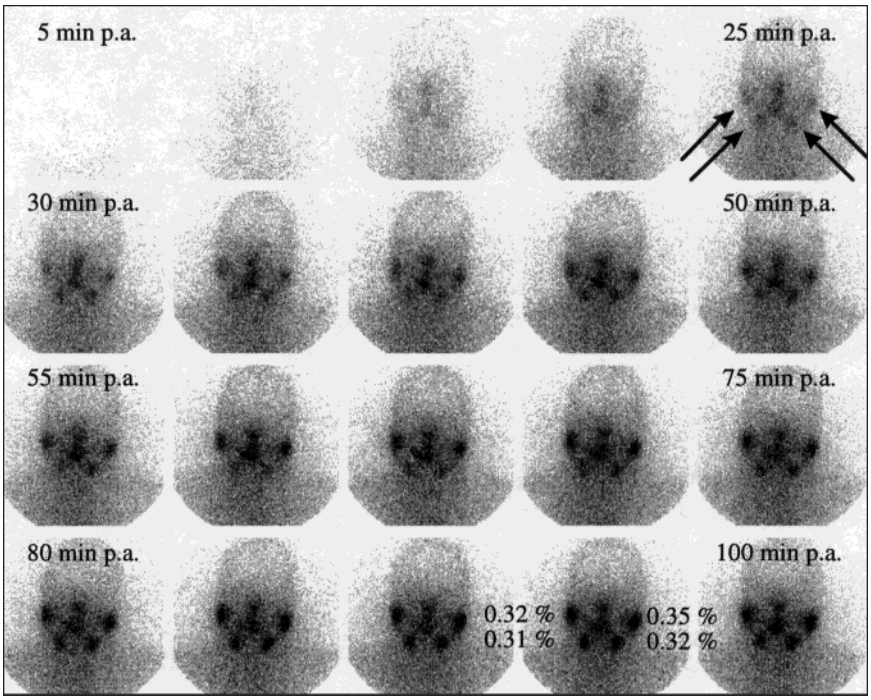

FIGURE 8. Sequential quantitative salivary gland scintigraphy started directly after the oral application of 400 MBq ^{131}I. Note the beginning accumulation of radioiodine in the salivary glands from as early as 25 min after oral application with increasing uptake over time.

CONCLUSION

Parenchymal damage in salivary glands induced by high-dose treatment was demonstrated to be significantly reduced by amifostine both in a rabbit animal model as well as in a patient study. Salivary gland scintigraphy is helpful in quantifying research of radioprotective drugs evaluating cytoprotective effects.

In addition, quantitative salivary gland scintigraphy may help to determine the optimal application time for radioprotective drugs. As shown in Figure 8, salivary glands begin to accumulate radioiodine as early as 25 min after oral application of ^{131}I. Thus, application of radioprotective drugs can be exactly correlated to radioiodine uptake to minimize parenchymal damage.

REFERENCES

1. Börner W. Speicheldrüsenfunktions- und Lokalisationsdiagnostik mit Radionukliden. In: Hundeshagen H, ed. *Nuclear Medicine*, Part 2 Diagnosis, Therapy, Clinical Research. Berlin, Germany: Springer; 1978:99–115.
2. Börner W, Grünberg H, Moll E. Die szintigraphische Darstellung der Kopfspeicheldrüsen mit technetium-99m. *Med Welt* (Stuttgart). 1965; 42:2378–2380.
3. de Rossi G, Galli G, Focacci C, Troncone L. Functional and morphological diagnosis of the salivary-gland diseases by means of radioisotopic methods. *Rad Diagn.* 1976; 17:409–419.
4. Kohn WG, Ship JA, Atkinson JC, et al. Salivary gland ^{99m}Tc-scintigraphy: a grading scale and correlation with major salivary gland flow rates. *J Oral Pathol Med.* 1992; 21:70–74.
5. Schall GL, Anderson LG, Wolf RO, et al. Xerostomia in Sjögren's syndrome. Evaluation by sequential salivary scintigraphy. *JAMA.* 1971; 216:2109–2116.
6. Schiodt M, Daniels TE, Greenspan JS, et al. Comparing diagnostic criteria for the salivary component of Sjögren's syndrome. *Scand J Rheumatol.* 1986; 61:44–46.
7. Schmitt G, Lehmann G, Strötges MW, et al. The diagnostic value of sialography and scintigraphy in salivary gland diseases. *Br J Radiol.* 1976; 49:326–329.
8. Sugihara T, Yoshimura Y. Scintigraphic evaluation of the salivary glands in patients with Sjögren's syndrome. *Int J Oral Maxillofac Surg.* 1988; 17:71–75.
9. Talal N. Sjögren's syndrome. *Bull Rheum Dis.* 1966; 16:404–407.
10. Albrecht HH, Creutzig H. Funktionsszintigraphie der Speicheldrüsen nach hochdosierter Radiojodtherapie. *Fortschr Röntgenstr.* 1976; 125:546–551.
11. Reiners C, Eilles C, Eichner R, et al. Speicheldrüsen-funktionsszintigraphie zur Verlaufskontrolle bei der Therapie des Schilddrüsen-Karzinoms mit Radiojod. *Nuklearmediziner.* 1980; 3:281–286.
12. Spiegel W, Reiners C, Börner W. Einschränkung der Speicheldrüsenfunktion nach hochdosierter Radiojodtherapie. *Nuklearmediziner.* 1986; 9:159–166.
13. Bornemann C, Creutzig H. Die klinische Bedeutung einer Speicheldrüsenszintigraphie. Eine Prospektive Studie. *HNO*. 1983; 31:200–206.
14. Drubach L, Lafrance ND, Kashima H, et al. Quantitative assessment of secretion of Tc-99m-pertechnetate in salivary gland disease [Abstract]. *J Nucl Med.* 1986; 27:1009.
15. Havlik E, Scherak O, Bergmann H, Kolarz G. Technetiumspeicherung der Parotis. Wertigkeit von Funktionsparametern beim Sjögren-Syndrom. *Nuklearmedizin.* 1976; 15:142–145.
16. Kolarz G, Bergmann H, Havlik E, et al. 99m-Tc-uptake der Parotis bei Sjögren-Syndrom. *Verh Dtsch Ges Rheumatol.* 1976; 4:498–503.
17. Liem IH, Olmos RAV, Balm AJM, et al. Evidence for early and persistent impairment of salivary gland excretion after irradiation of head and neck tumours. *Eur J Nucl Med.* 1996; 23:1485–1490.
18. Stephen KW, Robertson JW, Harden RM. Quantitative aspects of pertechnetate concentration in human parotid and submandibular salivary glands. *Br J Radiol.* 1976; 49:1028–1032.
19. van den Akker HP, Busemann-Sokole E. Absolute indications for salivary gland scintigraphy with ^{99m}Tc-pertechnetate. *Oral Surg Oral Med Oral Pathol*. 1985; 60:440–447.
20. Häusler RJ, Ritschard J, N'Guyen VT, et al. Differential diagnosis of xerostomia by quantitative salivary gland scintigraphy. *Ann Otol*. 1977; 86:333–341.
21. Börner W. Szintigraphische Darstellung der Kopfspeicheldrüsen. *Med Klin.* 1971; 66:1496–1501.
22. Lazarus JH, Stephen KW, Harden RM, et al. Simultaneous quantitative measurement of ^{131}I and ^{99m}Tc-pertechnetate uptake by human salivary glands using scintiscanning with validation by direct estimation in biopsy samples. *Eur J Clin Invest.* 1973; 3l: 156–159.
23. Daniels TE, Powell MR, Sylvester RA, Talal N. An evaluation of salivary scintigraphy in Sjögren's syndrome. *Arthritis Rheumatism.* 1979; 22:809–814.
24. Arrago JP, Rain JD, Rocher F, et al. Syndrome de Gougerot-Sjögren. Étude fonctionnelle des glandes salivaires par la scintigraphie. *Presse Med.* 1984; 13:209–213.
25. Lindvall AM, Jonsson R. The salivary gland component of Sjögren's syndrome: an evaluation of diagnostic methods. *Oral Surg Oral Med Oral Pathol*. 1986; 62:32–42.
26. Pilbrow WJ, Brownless SM, Cawood JI, et al. Salivary gland scintigraphy—a suitable substitute for sialography? *Br J Radiol*. 1990; 63:190–196.
27. de Rossi G, Focacci C. A computer-assisted method for semi-quantitative assessment of salivary gland diseases. *Eur J Nucl Med.* 1980; 5:499–503.
28. van den Akker HP, Busemann-Sokole E. Sequential scintigraphy of the salivary glands with special reference to the oral activity. *Int J Oral Surg.* 1974; 3:321–325.
29. Markusse HM, Pillay M, Cox PH. A quantitative index derived from ^{99m}Tc-pertechnetate scintigraphy to assist in the diagnosis of primary Sjögren's syndrome. *Nuklearmedizin.* 1992; 31:3–6.
30. Joseph K. Statische, dynamische und quantifizierte Schilddrüsenszintigraphie. *Nuklearmediziner.* 1979; 2:83–101.
31. Mahlstedt J. Statische und dynamische Schilddrüsenszintigraphie. *Nuklearmediziner.* 1986; 9:15–26.
32. Harden RM, Hilditch TE, Kennedy I, et al. Uptake and scanning of the salivary glands in man using pertechnetate-99m-Tc. *Clin Sci.* 1967; 32: 49–55.
33. Hug I, Holtgrave EA. Entzündliche Erkrankungen der Parotis—Korrelation von Sialographie und Funktionsszintigraphie. *Laryng Rhinol.* 1974; 53:213–222.
34. Schall GL, Larson SM, Anderson LG, Griffith JM. Quantification of parotid gland uptake of pertechnetate using a gamma scintillation camera and a ''region-of-interest'' system. *Am J Roentgenol Radium Ther Nucl Med.* 1972; 115:689–697.
35. Schneider P, Traurig G, Haas JP. Quantitative Funktionsszintigraphie der Speicheldrüsen. I. Die Bestimmung der globalen und regionalen Drusenfunktion. *Fortschr Röntgenstr.* 1984; 140:93–96.
36. Spens E, Dietzel C, Klaua M, Grimm D. Computerszintigraphische Untersuchungen zur Funktion der grossen Kopfspeicheldrüsen. *Stomatol DDR.* 1990; 40:52–54.
37. Stephen KW, Chisholm DM, Harden RM, et al. Diagnostic value of quantitative scintiscanning of the salivary glands in Sjögren's syndrome and rheumatoid arthritis. *Clin Sci*. 1971; 41:555–561.
38. Vigh L, Carlsen O, Hartling OJ. Uptake index and stimulated salivary gland response in ^{99m}Tc-pertechnetate salivary gland scintigraphy in normal subjects. *Nucl Med Commun.* 1997; 18:363–366.
39. Bohuslavizki KH, Brenner W, Tinnemeyer S, et al. Quantitative salivary gland scintigraphy derived from 166 normals. *Radiol Oncol*. 1995; 29:297–305.
40. Bohuslavizki KH, Brenner W, Wolf H, et al. Value of quantitative salivary gland scintigraphy in the early stage of Sjögren's syndrome. *Nucl Med Commun.* 1995; 16:917–922.
41. Bohuslavizki KH, Brenner W, Lassmann S, et al. Quantitative salivary gland scintigraphy in the diagnosis of parenchymal damage after radioiodine [Abstract]. *Eur J Nucl Med*. 1996; 23:1062.
42. Bohuslavizki KH, Brenner W, Lassmann S, et al. Die quantitative Sialoszintigraphie—eine sinnvolle Untersuchung im Vorfeld und in der Nachsorge der Radiojodtherapie. *Nuklearmedizin.* 1997; 36:103–109.
43. Bohuslavizki KH, Brenner W, Tinnemeyer S, et al. Is quantitative salivary gland scintigraphy a mandatory examination prior to and after radioiodine therapy. *Radiol Oncol*. 1997; 31:5–12.
44. Becker DV, Hurley JR. Radioiodine treatment of hyperthyroidism. In: Sandler MP, Patton JA, Coleman RE, et al, eds. *Diagnostic Nuclear Medicine*, 3rd ed. Baltimore, MD: Williams & Wilkins; 1995:943–958.
45. Becker DV, Hurley JR. Treatment of thyroid cancer with radioiodine (^{131}I). In: Sandler MP, Patton JA, Coleman RE, et al, eds. *Diagnostic Nuclear Medicine*, 3rd ed. Baltimore: Williams & Wilkins; 1995:959–989.

46. Bender JM, Dworkin HJ. Therapy of hyperthyroidism. In: Henkin RE, Boles MA, Dillehay GL, et al, eds. *Nuclear Medicine*. St Louis, MO: Mosby; 1996:1549–1567.
47. Johannsson L, Mattsson S, Nosslin B, Leide-Svegborn S. Effective dose from radiopharmaceuticals. *Eur J Nucl Med.* 1992; 19:933–938.
48. Bohuslavizki KH, Brenner W, Lassmann S, et al. Quantitative salivary gland scintigraphy in the diagnosis of parenchymal damage after treatment with radioiodine. *Nucl Med Commun.* 1996; 17:681–686.
49. Arnett FC, Edworthy SM, Bloch DA, et al. The American Rheumatism Association 1987 revised criteria for the classification of rheumatoid arthritis. *Arthritis Rheum.* 1988; 31:315–324.
50. Manthorpe R, Oxholm P, Prause JU, Schiodt M. The Copenhagen criteria for Sjögren's syndrome. *Scand J Rheumatol.* 1986; 61 (suppl):19–21.
51. Sodicoff M, Conger AD, Trepper P, Pratt NE. Short-term radioprotective effects of WR-2721 on the rat parotid glands. *Radiat Res.* 1978; 75:317–326.
52. Sodicoff M, Conger AD, Pratt NE, Trepper P. Radioprotection by WR-2721 against long-term chronic damage to the rat parotid gland. *Radiat Res.* 1978; 76:172–179.
53. Menard TW, Izutsu KT, Ensign WY, et al. Radioprotection by WR-2721 of gamma-irradiated rat parotid gland: effect on gland weight and secretion at 8–10 days post irradiation. *Int J Radiat Oncol Biol Phys.* 1984; 10:1555–1559.
54. Pratt NE, Sodicoff M, Liss J, et al. Radioprotection of the rat parotid gland by WR-2721: morphology at 60 days post-irradiation. *Int J Radiat Oncol Biol Phys.* 1980; 6:431–435.
55. Bohuslavizki KH, Brenner W, Hübner R, et al. Protective effect of amifostine on salivary glands of rabbits treated with high dose iodine-131 [Abstract]. *J Nucl Med.* 1997; 38:223P-224P.
56. Bohuslavizki KH, Brenner W, Hübner R, et al. Zytoprotektion durch Amifostin bei I-131-induzierter Schädigung in Kaninchenspeicheldrüsen [Abstract]. *Nuklearmedizin.* 1997; 36:3.
57. Bohuslavizki KH, Brenner W, Tinnemeyer S, et al. Zytoprotektion der Speicheldrüsen durch Amifostin bei Gabe von 6 GBq I-131—erste Ergebnisse [Abstract]. *Nuklearmedizin*. 1997; 36:3.
58. Bohuslavizki KH, Brenner W, Lassmann S, et al. Wirksamkeit von Amifostin zur Zytoprotektion der Speicheldrüsen bei Gabe von 6 GBq I-131 [Abstract]. *Nuklearmedizin.* 1997; 36:1.
59. Bohuslavizki KH, Brenner W, Klutmann S, et al. Radioprotection of salivary glands by amifostine in high-dose radioiodine therapy. *J Nucl Med.* 1998; 39:1237–1242.